ELSEVIER

Earth and Planetary Science Letters 210 (2003) 467–479

EPSL

www.elsevier.com/locate/epsl

The Paleoproterozoic McArthur River (HYC) Pb/Zn/Ag deposit of northern Australia: organic geochemistry and ore genesis

Junhong Chen [a,b], Malcolm R. Walter [a,*], Graham A. Logan [a,b], Mark C. Hinman [c], Roger E. Summons [a,b,1]

[a] *Australian Centre for Astrobiology, Department of Earth and Planetary Sciences, Macquarie University, Sydney, NSW 2109, Australia*

[b] *Geoscience Australia, GPO Box 378, Canberra, ACT 2601, Australia*

[c] *HINMAN GeoSOLUTIONs, 43 Gerler Street, Bardon, Brisbane, Qld 4065, Australia*

Received 29 May 2002; received in revised form 24 January 2003; accepted 21 March 2003

Abstract

Polycyclic aromatic hydrocarbons (PAHs) in ore and mudstone within the McArthur River ore deposit show compound distribution patterns similar to those of hydrothermally generated petroleum in the Guaymas Basin and significantly different from those found in conventional oil. PAH abundances and their isomer distributions result from a temperature gradient between the source of mineralizing fluids and the sediments fringing the ore system during ore formation. Along with other geochemical, geological, paleobiological and mineralogical lines of evidence, these data provide strong evidence that the ore formed within partially lithified sediments under marine conditions. Given that the McArthur River ore body is an exquisitely preserved example of a sediment-hosted base-metal deposit, these results may be widely applicable. The McArthur deposit is also a rich repository of paleobiological information, allowing studies of the microbiology of ore formation and the paleobiology of an ancient hydrothermal system, as is discussed elsewhere.

Keywords: hydrothermal ore deposit; organic geochemistry; Proterozoic; Australia; McArthur River

1. Introduction

The 1640 Ma McArthur River (HYC) lead–zinc–silver deposit of northern Australia is the largest known stratiform sediment-hosted base-metal deposit. It is extraordinarily well preserved, with all indicators of burial maturity indicating that the host rocks have experienced temperatures only up to the window of oil generation [1]. The

* Corresponding author. Tel.: +61-2-98508354; Fax: +61-2-98508248.
E-mail address: malcolm.walter@mq.edu.au (M.R. Walter).

[1] Present address: Department of Earth Atmospheric and Planetary Sciences, MIT, Cambridge, MA 02139-4307, USA.

0012-821X/03/$ – see front matter
doi:10.1016/S0012-821X(03)00171-7

deposit has been intersected by more than 100 drill holes, and is exposed in an underground mine. This accessibility has afforded superb opportunities for detailed studies [2–10]. Despite this, interpretations of the genesis of the ore vary widely, with three end-member models proposed: syngenetic (exhalative) in a deep marine setting [3,10]; 'early diagenetic' within the mud and silt of an ephemeral lake/sahbka environment [4,5]; and sub-sediment–water interface ('early diagenetic') in a marine environment below wave base [8,9]. We show here that organic geochemistry can help resolve differences between these models of ore genesis.

As part of a continuing study of the deposit [1], we have conducted analyses of hydrocarbons from the ore and from associated sediments sampled on a centimeter to millimeter scale (for example, see Fig. 1). We have also analyzed the $\delta^{13}C$ composition of selected hydrocarbons in both mineralized and unmineralized horizons to help determine their biological origins. Microfossils have been identified in the ore deposit [11,12], and we have supplemented the published work with observations from splits of the samples used in our organic geochemical analyses. Some initial results of our biomarker and microfossil work are published elsewhere [1]. Here we present analyses of polycyclic aromatic hydrocarbons (PAHs) particularly relevant to determining the thermal history of the ore and its host sediments. Our results impact significantly on the capacity to distinguish between alternative ore genesis models.

2. Geological setting

The McArthur River deposit formed within the McArthur Basin, an intracratonic basin resting on a basement of Paleoproterozoic granites and metamorphic rocks. Mineralized zones occur in the HYC Pyritic Shale Member of the Barney Creek Formation within the largely platformal McArthur Group, which was deposited within a tectonically induced sub-basin with its eastern boundary located along the syn-depositional Emu Fault Zone (Fig. 2). The host rocks to the ore horizons are dark, carbonaceous and pyritic dolomitic graded siltstones and mudstones, with abundant graded breccias of pre-Barney Creek dolomite [2,13]. The siltstones have parallel laminae 0.5–50 mm thick, locally with small-scale cross-lamination, scour and fill, graded textures and slumping [2,10,13,14]. The HYC Pyritic Shale Member is thickest west of the Emu Fault and the Western Fault Block and thins over, and lies unconformably on, domes or fault blocks across the region [13]. Evidence for syn-depositional faulting and tilting comes from the graded sedimentary breccias that coarsen and thicken northwards [8]. There are dolostone clasts of recognizable origin within the breccias, derived from the upthrown fault blocks within the Emu Fault Zone and evidencing the progressive exhumation of the entire McArthur Group during Barney Creek time [13]. The coarse detrital rocks range from graded dolarenite beds a few millimeters thick, to massive breccias with clasts up to several meters wide. Most are thought to have been deposited from flows moving in a predominantly southerly to southwesterly direction [8,9,13].

Mineralization consists mostly of pyrite, sphalerite and galena, in varying proportions, finely disseminated throughout the siltstone. Ore-rich laminae are commonly enclosed between layers of poorly mineralized to unmineralized mudstone and siltstone. Sulfide concentrations within ore laminae are commonly greater than 60% by weight [2,9]. Unmineralized layers are present throughout the succession and vary in thickness from millimeter-scale mudstone layers, centimeter-scale turbidites to meter-scale breccia beds. Isolation of the centimeter-scale turbidite beds is possible using a rock saw and this approach was used to examine organic geochemical differences at a centimeter scale between mineralized and unmineralized sediments within the ore deposit. Isotopic analysis and detailed study of the mineral textures have shown that the ore body contains several phases of sulfide [15]. Those authors suggested that an early diagenetic pyrite phase (Py 1) was generally followed by a later and more massive pyrite phase (Py 2) and that this, in turn, was further over-printed by sphalerite and galena. Py 1 has $\delta^{34}S$ values consistent with formation by

bacterial sulfate reduction (BSR) in a system open to sulfate, and probably formed at, or close to, the sediment–water interface. Py 2 is enriched in ^{34}S relative to coexisting Py 1 and this has been explained as resulting from later closed-system reduction within the sediment pile [15] or by the incorporation of excess heavy sulfate, within the BSR pyrite zone immediately beneath the sediment–water interface, in the outflow zone of the sub-surface mineralizing system [9]. Based on SHRIMP measurements, $\delta^{34}S$ values for galena and sphalerite range between -5 and $+5‰$. This mineralization is thought to have involved reaction of sulfate in the hydrothermal ore solution with organic matter in the Barney Creek Formation [4,9]. The ore-forming fluid has been considered to have been a moderately hot (150–250°C), oxidized (sulfate > sulfide) brine, rich in sulfate and metals, at the point where it entered the basin [9,10]. The low metal-carrying capacities of brines in that temperature range require there to have been a large volume of oxidized fluid sourced from an evaporite deposit. However, our new data suggest another possibility that we present below.

3. Materials and methods

Nine rock samples were selected for analysis from those collected from the McArthur River Mine. Some samples are of a single lithology (e.g. 2H9/1B 1/2-mudstone). Most samples are comprised of several different lithologies, and those were separated before the detailed study of aromatic hydrocarbon distributions. For example, sample 2E4/G 1 was separated into three sub-samples: chert nodules, carbonate-rich mudstone around chert nodules and ore, and sample 2H9/1C was separated into two ore sub-samples (ore#1 and #2) and two mudstone sub-samples (mud#1 and #2). Fig. 1 illustrates some samples in their original state, before separation of different lithologies.

3.1. Sample processing

Samples were cut with a diamond saw along lithological boundaries. Adhering portions of other lithologies were removed by grinding. The saw coolant was tap water. The analysis of sample blanks demonstrated that there were no significant contaminants.

Chert had to be separated by a different technique because it occurs as small nodules (2 mm to 1 cm) in a carbonate-rich mudstone. These samples were cut into small pieces with and without chert nodules and the pieces with chert nodules were crushed into particles of about 2 mm in size using a ball mill. The crushed samples were then washed with distilled water to remove fine powder. The particulate chert material was then treated with 10 M HCl solution to remove any carbonate and then washed with distilled water to pH = 7, then dried at room temperature. Chert particles were selected under a microscope before analysis. The pure chert particles (and all the other samples) were washed with dichloromethane (DCM) three times to remove possible organic contamination obtained during sample processing. After the DCM evaporated, the samples were crushed to powder with the ball mill.

3.2. Extraction and separation

Before extraction all samples were washed as described above. Isolation of extractable organic matter (EOM) derived from core and from rock samples from faces within the mine was conducted in a Sohxlet apparatus with DCM for 72 h. Elemental sulfur was removed using activated copper chips in the extraction vessel. The solvent was then concentrated and half of the EOM was used for gas chromatography (GC) and gas chromatography–mass spectrometry (GC–MS) analysis. The second half of the total extract was further separated into two equal parts: the first quarter was concentrated into 50–100 μl and an internal standard (d14-terphenyl) was added, before GC and GC–MS quantification analysis. The second quarter of the total extract was then separated into saturates, aromatics and polar fractions using silica gel column chromatography with petroleum ether, mixtures of DCM and petroleum ether (50:50) and DCM and methanol (50:50) as eluting solvents respec-

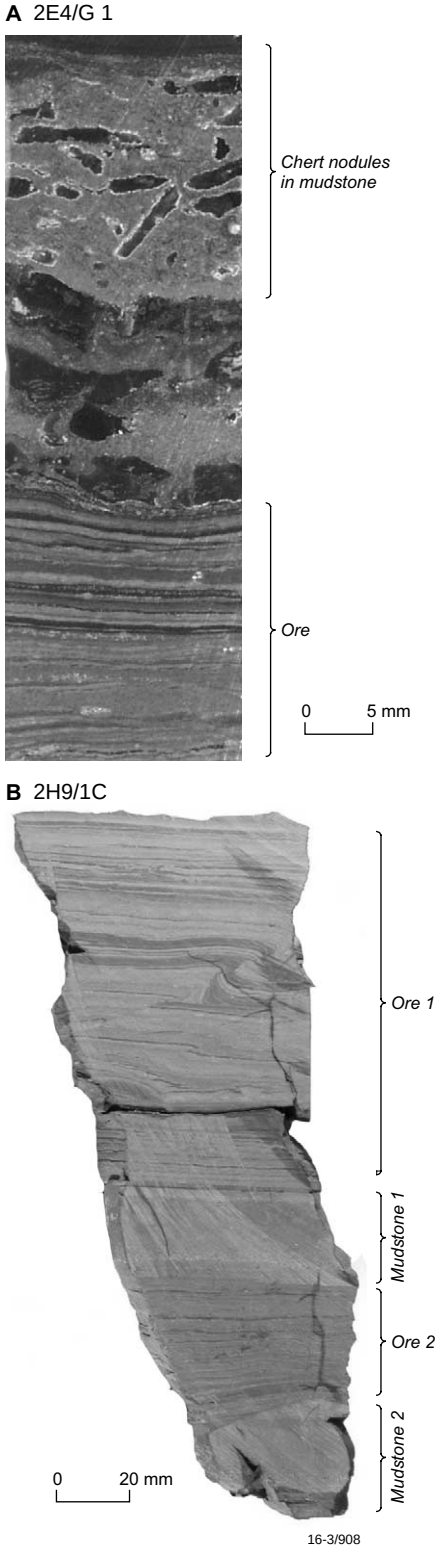

tively. The aromatic fractions were then used for GC and GC–MS analysis.

3.3. GC analysis

GC was carried out on a Hewlett Packard HP6890 series gas chromatograph with HP Chemstation software. Injections were made using splitless injection and a 25 m × 0.25 mm i.d. capillary column, with DB-1 stationary phase and He carrier gas, programmed at 60°C for 2 min, then ramped at 4°C/min to 310°C and then held isothermally for 20 min.

3.4. GC–MS analysis

GC–MS was carried out on a HP mass-selective detector attached to an HP 6890 series GC using a 50 m × 0.25 mm i.d. fused silica tubular column coated with a 0.25 μm DB-5 stationary phase (J&W Scientific) and He carrier gas in a splitless injection mode. The GC was held isothermal at 40°C for 2 min, followed by a temperature increase at 4°C/min, and an isothermal period of 20 min at the upper temperature of 320°C. During full-scan acquisition the mass spectrometer was operated in the electron ionization mode scanning from *m/z* 50–600, with a scan time of 1.0 s and electron energy of 70 eV.

Perdeuterized terphenyl (d14, molecular weight = 244) was used as the internal standard for quantification of individual compounds. The absolute concentration of each was normalized to the total organic carbon (ng/g TOC or ppb).

3.5. TOC analysis

Analyses of TOC were done with a Rock Eval 6.

←

Fig. 1. Photograph of two samples used in the analysis of McArthur River ore. The chert nodules were isolated from carbonate matrix during analysis.

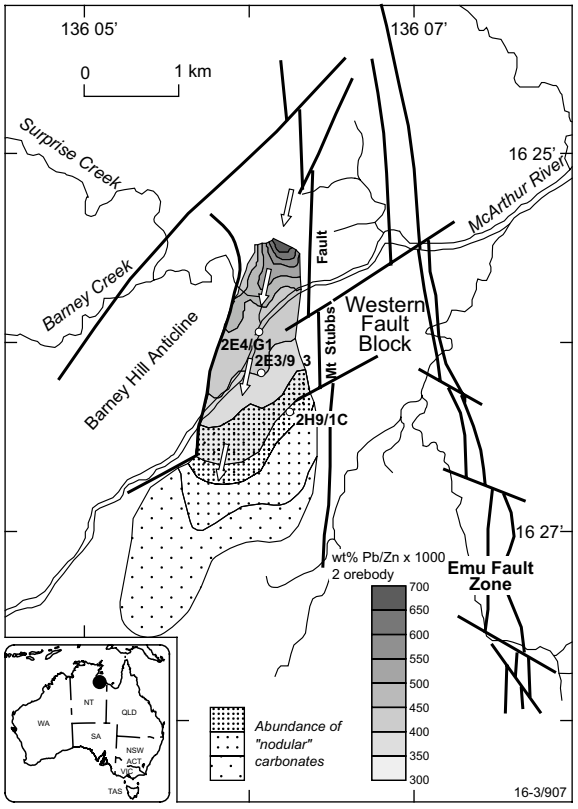

Fig. 2. Map of the McArthur River mine showing sample locations and metal ratios. Hypothesized flow of the mineralizing brine is indicated by arrows.

4. Results and discussion

4.1. Aromatic hydrocarbons

As some of the models for the formation of the McArthur deposit involve warm to hot mineralizing fluids interacting with organic matter we compared bitumen components of the deposit with modern analogs where there are fluids with elevated temperatures. In modern marine hydrothermal systems, such as the Guaymas Basin (Gulf of California) and Middle Valley (Juan de Fuca Ridge), hydrothermal bitumens have been found to have distinctive geochemical signatures. In particular, the bitumens contain characteristic patterns of PAHs with low levels of alkylation and increased abundances of large, multi-ring members such as benzopyrene, benzoperylene and coronene [16,17]. The rapid heating rates developed during the interaction of hot brines and organic matter are thought to favor the formation of non-alkylated and highly condensed PAHs. Elevated abundances of PAHs have been observed not only in modern hydrothermal petroleum systems such as those of Guaymas and Middle Valley, but also in ancient mineral systems such as Red Dog Zn–Pb mine, Northwest Alaska [18] and Kupferschiefer Shale (Cu–Zn–Pb) in Europe [19,20].

We sampled within a single ore body exposed within the mine to obtain large, pristine samples for geochemical analysis (Fig. 1). Three separate sites were selected (Fig. 2) and several lithologies at each site were examined. The sample sites reflect different temperature regimes during ore formation within the ore body as indicated by lead to zinc ratios. The northern sample sites 2E4/G 1 and 2E3/9 3 are thought to be closest to the source of hot mineralizing brine. The southern

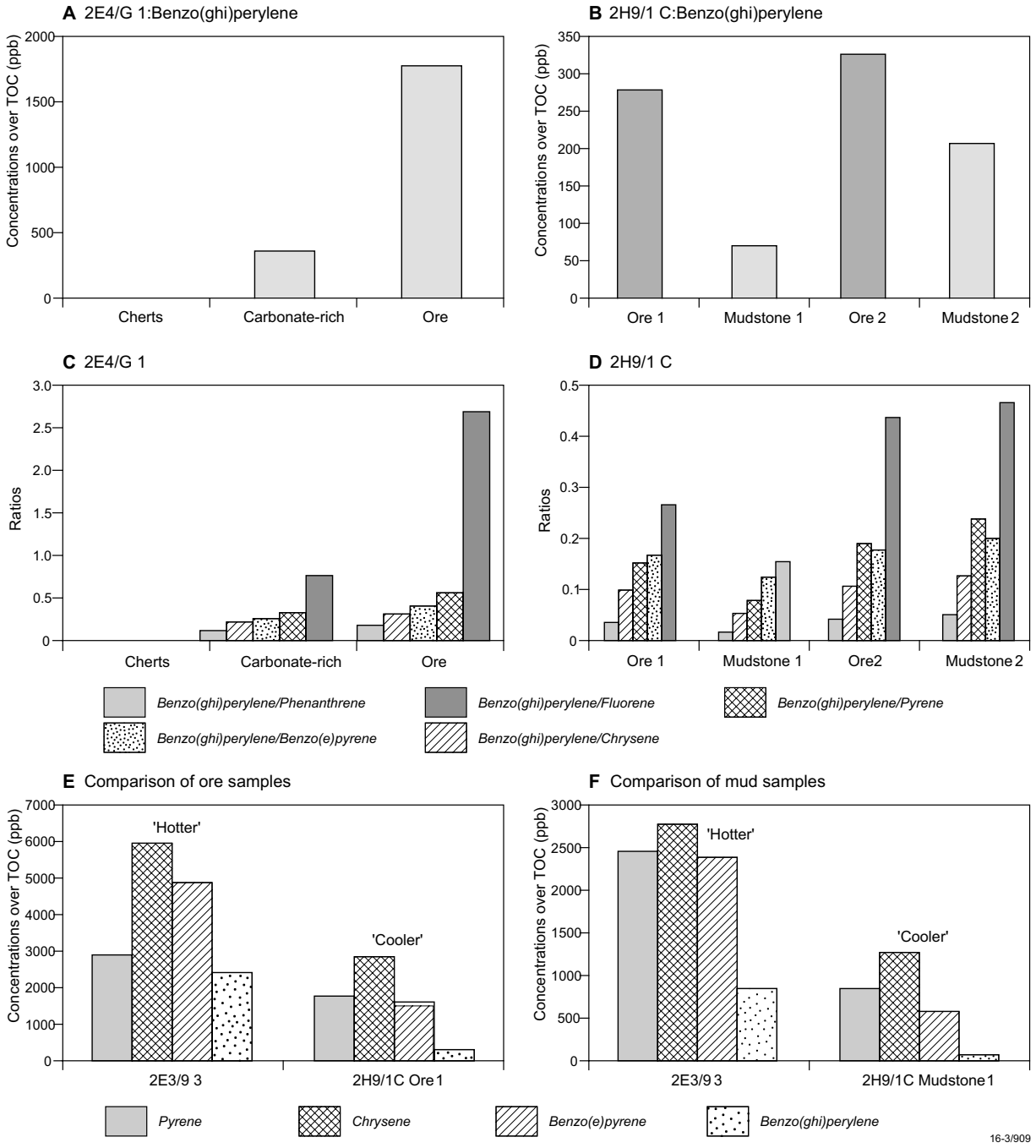

Fig. 3. Histograms of abundances and ratios of key aromatic compounds used in this study. Diagrams A and B display the abundance of benzo(ghi)perylene in sample 2E4/G 1 from the 'hotter' area and sample 2H9/1C from the 'cooler' area. Diagrams C and D display the ratio of benzo(ghi)perylene to other smaller PAH compounds in 2E4/G 1 and 2H9/1C. The abundances and ratios are higher in ores than other lithologies. Note the difference in scale between diagrams A and B, and C and D. The abundances of PAHs within ores and muds from different areas were compared, showing that samples from the 'hotter' area are richer in PAHs (diagrams E and F).

Table 1
Quantified aromatic compounds and ratios for samples reported in this study

Sample	19990673			19990675			20000123			
Original ID	2E4/G 1			2E3/9 3			2H9/1C			
Description	cherts	carbonate-rich part	ore	crust	mud	ore	ore#1	mud#1	ore#2	mud#2
TOC (%)	0.05	0.90	0.51	0.11	0.86	0.88	0.53	0.59	0.45	0.75
Compounds	ppb over TOC									
Phenanthrene	6 343.02	3 691.76	9 921.58	7 071.52	10 889.04	9 475.59	7 735.10	4 204.14	7 635.29	4 027.45
3-Methylphenanthrene	5 941.63	3 244.22	13 076.24	6 693.12	11 121.58	11 253.02	6 474.85	3 365.34	6 433.97	3 267.24
2-Methylphenanthrene	6 579.24	3 873.97	15 700.98	8 305.29	14 058.33	14 931.67	8 381.90	4 387.79	8 531.09	4 323.77
9-Methylphenanthrene	4 259.62	1 794.03	8 149.98	4 997.83	6 966.15	6 788.00	3 285.74	1 671.93	3 161.06	1 623.88
1-Methylphenanthrene	2 287.21	1 219.98	6 799.36	3 797.27	6 499.26	6 036.57	2 594.79	1 329.01	2 527.11	1 290.93
Methylphenanthrenes	19 067.69	10 132.20	43 717.55	23 793.52	38 645.32	39 009.26	20 737.28	10 754.07	20 653.23	10 505.83
Tetramethylnaphthalenes	4 798.21	800.08	6 481.98	4 515.90	5 231.83	6 488.15	1 063.81	451.04	926.27	445.91
Dibenzothiophene (DBT)	558.70	99.59	286.48	584.64	955.15	686.05	231.20	118.36	208.60	133.13
4-Methyl-DBT	0.00	163.65	71.11	1019.82	1750.96	1325.61	329.60	163.34	309.24	186.45
2+3-Methyl-DBT	0.00	84.51	540.81	531.37	1 155.31	711.95	186.94	93.86	184.14	109.68
1-Methyl-DBT	0.00	23.72	184.59	243.95	413.52	156.59	35.87	20.22	33.42	23.86
MDVTs	0.00	271.88	1 436.52	1 795.13	3 319.79	2 194.16	552.42	277.42	526.80	319.98
Fluorene	1 045.74	469.12	667.24	385.24	753.17	1 001.79	824.97	452.57	741.14	437.88
Pyrene	2 216.72	1 104.27	3 257.64	1 883.00	2 443.29	2 896.83	1 798.84	843.82	1 664.42	864.98
Chrysene	2 531.29	1 827.93	5 676.69	2 836.33	2 787.94	5 959.09	2 835.17	1 278.20	3 108.80	1 585.54
Benzo(e)pyrene	0.00	1 431.93	4 924.85	1 472.68	2 404.31	4 911.75	1 640.06	576.63	1 858.96	1 026.24
Benzo(ghi)perylene	0.00	353.37	1 790.11	706.58	880.09	2 432.22	273.54	69.08	324.79	203.69
Coronene	0.00	18.75	374.68	0.00	83.87	573.82	12.73	0.00	16.96	9.54
Ratios										
MPI	1.52	1.67	1.80	1.48	1.62	1.68	1.72	1.70	1.78	1.73
Benzo(e)pyrene/Pyrene	0.00	1.30	1.51	0.78	0.98	1.70	0.91	0.68	1.12	1.19
Benzo(e)pyrene/Chrysene	0.00	0.78	0.87	0.52	0.86	8.26	0.58	0.45	0.60	0.65
Chrysene/Fluorene	2.42	3.90	8.51	7.36	3.70	5.95	3.44	2.82	4.19	3.62
Chrysene/Phenanthrene	0.40	0.50	0.57	0.40	0.26	0.51	0.37	0.30	0.41	0.39
Benzo(ghi)perylene/Phenanthrene	0.00	0.10	0.18	0.10	0.08	0.21	0.04	0.02	0.04	0.05
Benzo(ghi)perylene/Pyrene	0.00	0.32	0.55	0.38	0.36	0.84	0.15	0.08	0.20	0.24
Benzo(ghi)perylene/Fluorene	0.00	0.75	2.68	1.83	1.17	2.43	0.33	0.15	0.44	0.47
Benzo(ghi)perylene/Chrysene	0.00	0.19	0.32	0.25	0.32	4.09	0.10	0.05	0.10	0.13
Benzo(ghi)perylene/Benzo(e)pyrene	–	0.25	0.36	0.48	0.37	0.50	0.17	0.12	0.17	0.20

sample site 2H9/1C, although highly mineralized, is thought to represent a cooler zone and is further from the source of brine at 2 ore-body level (Fig. 2). We examined the aromatic hydrocarbons in each of the samples for evidence of preserved hydrothermal signatures. We also examined hydrocarbon biomarker distributions in the same samples for paleoenvironmental signals.

The ores at sites 2E4G/G1 and 2E3/9 3 (both in 'hotter' zones) are rich in PAHs relative to other lithologies centimeters to decimeters distant at these sites. In particular, pyrene, benzo(e)pyrene, benzo(ghi)perylene and chrysene are two to three times more abundant in ore relative to enclosing lithologies (Table 1). For example, benzo(ghi)perylene (a compound with six benzene rings) has concentrations of 1790 ppb in ore and 353 ppb in associated carbonate-rich rocks, and is absent in associated chert (Fig. 3A). These large, highly condensed PAHs are enriched in petroleums of hydrothermal origin [16,17]. Furthermore, values for the ratios of high molecular weight to lower molecular weight parent (unsubstituted) PAHs are much greater within the ore horizons compared with contiguous sedimentary rocks (Fig. 3B and Table 1).

Ores at site 2H9/1C ('cooler' zone) also show similar trends to those from the 'hotter' zones of mineralization when compared to their enclosing rocks (Fig. 3C,D). However, concentrations of unsubstituted PAHs are significantly lower (Fig. 3E and Table 1). Muddy lithologies consisting of unmineralized dolomitic graded beds of centimeter thicknesses associated with the ores at sites 2E3/9 3 and 2H9/1C also exhibit similar trends to the ore horizons, with decreasing abundances of unsubstituted PAHs in the cooler zones (Fig. 3F and Table 1). These observations are consistent with the precipitation of PAHs in the ore horizons at each site and the existence of a large thermal gradient between sites. This would suggest that the PAHs were generated upstream and moved laterally with the mineralizing brine. As the brine cooled and the solubility of the PAHs dropped, they were precipitated out of solution in order of their molecular weight (as is further discussed later in this section). The preserved distribution reflects this migration and cooling trend, and also indicates that ore-forming fluids were predominantly confined between muddy beds. The confining beds contain significantly lower concentrations of hydrothermally generated PAHs, although the presence of low quantities within the enclosing sediments does suggest a degree of fluid mobility between ore and mud horizons.

The methyl phenanthrene index (MPI) is a molecular maturity parameter commonly used in petroleum exploration to assess the relative maturities of sediments and oils. The values of MPI for McArthur River samples range from 1.68% to 1.80% for ores and from 1.48% to 1.73% for surrounding rock types (Table 1), indicating that those samples are all thermally mature and suggesting that the ores have experienced higher temperatures relative to associated sediments at each site. In modern hydrothermal systems, PAH compositions are marked by low levels of alkylation. This is not observed in lower molecular weight PAHs from the ore body. We believe that this is due to the overprinting of the hydrothermally generated signal with the in situ production of aromatic hydrocarbons from residual organic matter during normal burial maturation. This mixture of hydrocarbons leads to the very unusual circumstance of different methylphenanthrene distributions in closely spaced samples. This is particularly apparent in the hotter 2E4G1 and 2E3/93 samples (Table 1).

Comparison of interbedded mudstone and ore at site 2H9/1C shows that the ore is consistently enriched in sulfur-containing organic compounds. This is also the case at site 2E4/G 1, where the ore is also enriched compared to other lithologies (Table 1). At site 2E3/9 3 all samples are enriched in sulfur-containing compounds with both the ore and mudstone horizons exhibiting the highest concentrations of these compounds among all samples analyzed. Thus, the highest overall abundances of these compounds, and hence the degree of sulfurization of organic matter, correlate not only with the presence of ore but also the presumed temperature profile across the deposit.

The suite of aromatic hydrocarbons found most abundantly in the ore, but also in its host rocks, is closely comparable with that found in the hydrothermally generated petroleums of the Guaymas

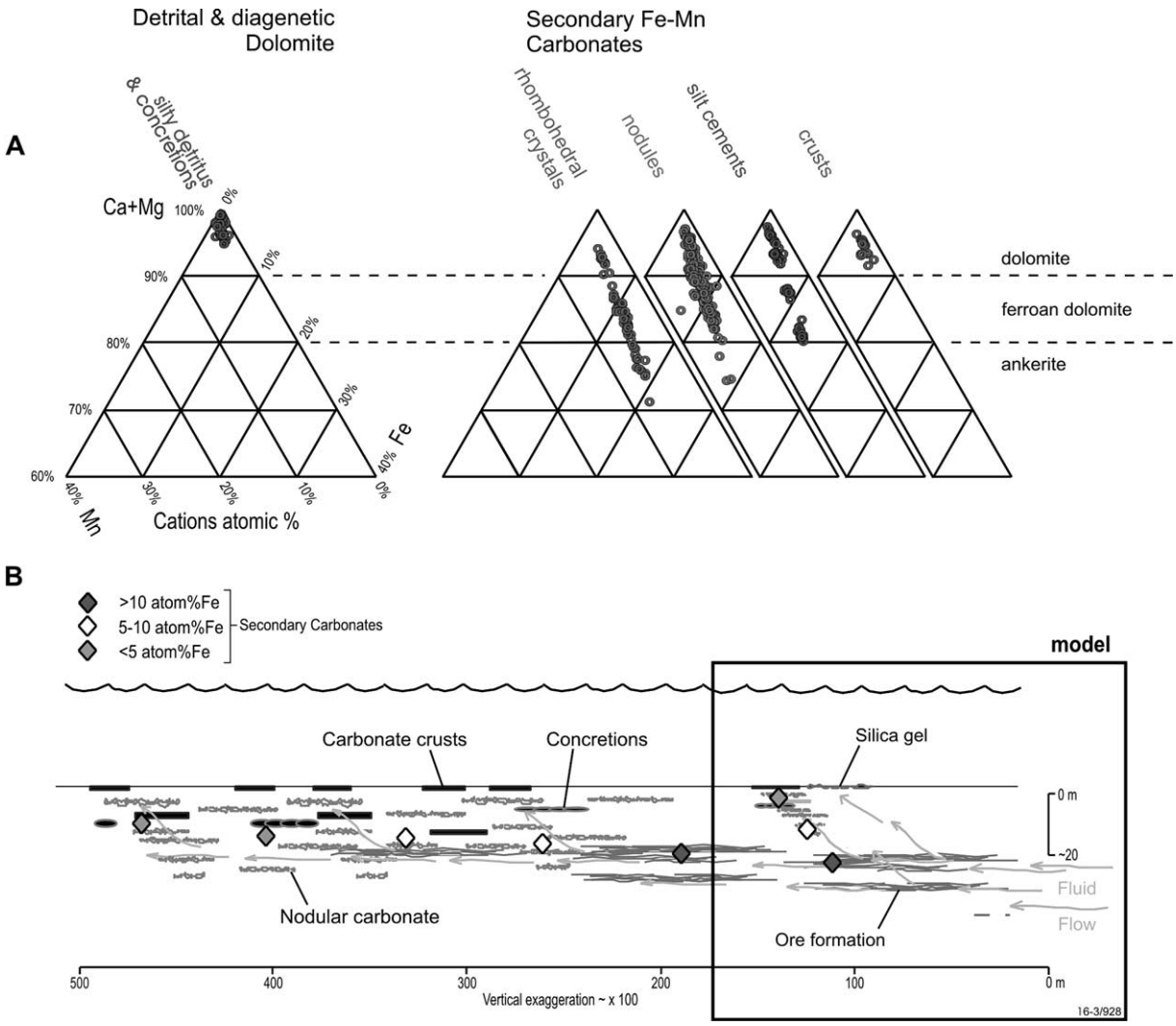

Fig. 4. Secondary carbonates are strongly enriched in Fe and Mn (A) and show vertical and lateral zoning (B). The Fe–Mn concentration of carbonates decreases away from the site of primary dissolution. This zoning can be readily explained by the relatively lower solubility of Fe–Mn-rich carbonates. Sediments unaltered by dissolution reactions within silty beds and carbonate concretions do not exhibit Fe or Mn enrichment. The boxed component of the figure refers to Fig. 5, where greater detail is shown.

Basin and Middle Valley studied by Simoneit [17]. The compound distributions are considered to be diagnostic for systems in which organic matter is rapidly heated during the passage of hot water through sediments, as opposed to distributions formed during low-temperature diagenesis or normal burial maturation. Moreover, they do not occur at other locations in the McArthur Basin, away from the ore bodies [21]. In the Guaymas Basin, vented fluids containing hydrothermally generated PAHs have temperatures greater than 300°C. Furthermore, sealed hydrous pyrolysis experiments indicate that these compounds form between 250 and 400°C (Simoneit, personal communication, 2001). This suggests that the ore-forming brine may have been significantly hotter than the previous estimates of between 150 and 250°C. Temperatures of >250°C would greatly increase

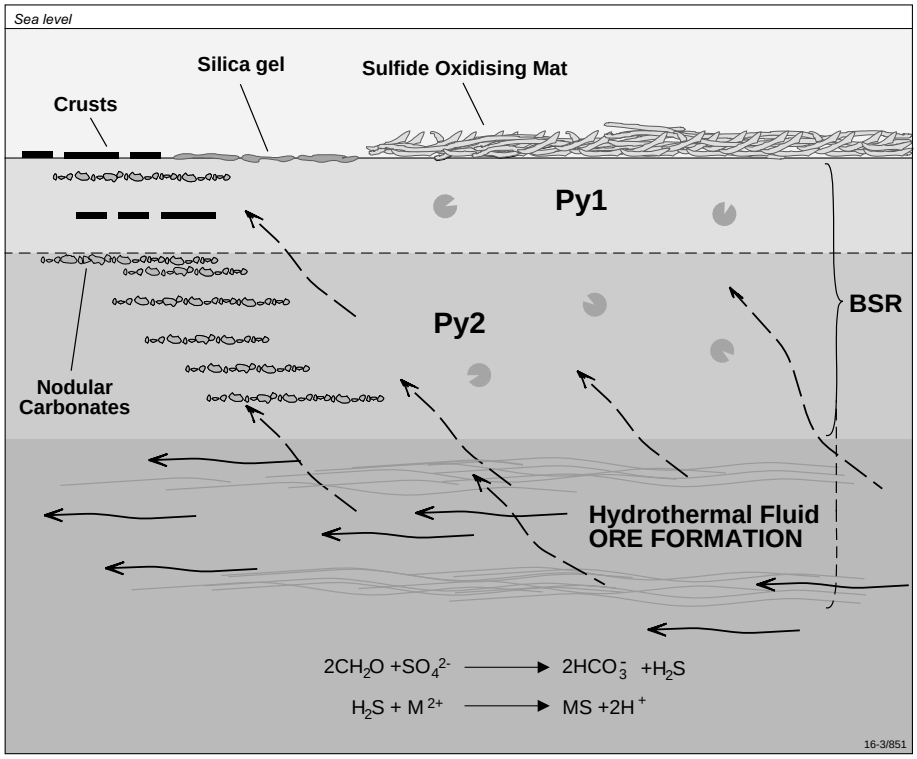

Fig. 5. Model of the mineralization process at McArthur River [1]. BSR is responsible for production of biogenic pyrite (Py 1 and Py 2). Sub-surface reaction between a hydrothermal brine rich in metals and sulfate with organic matter produces metal sulfides and bicarbonate. This reaction may be by thermochemical sulfate reduction in the hotter zones of the brine flow path but most likely is mediated by BSR in cooler zones. The bicarbonate generated during reaction is precipitated as nodular carbonate downstream (see Figs. 2 and 4) and above the ore formation zone as 'nodular carbonate' and carbonate 'crusts' at the sediment–water interface. Silica gel is also deposited at the sediment–water interface from outflowing brine. At the higher temperatures proposed here sulfide may also have been carried in the ore-forming brine. Communities of sulfide-oxidizing bacteria form after oxygenation of the water column caused by turbidite deposition and derive sulfide from the sediments.

the metal-carrying capacity of the brine and would allow sulfide to be present in the ore fluids. This has major implications for the ore genesis and exploration models, as the brine would have to have been generated in deeper areas of the basin and evaporites would not be required as a source of sulfate. Catalytic effects by metals may reduce these temperature estimates somewhat; however, a temperature of 250–300°C would be sufficient to generate all the characteristics we have outlined.

4.2. Ore genesis

Recent sedimentological studies indicate that the HYC Pyritic Shale was deposited in an intracratonic marine environment below wave base [10,22]. Our saturated hydrocarbon biomarker results also indicate a marine environment [1]. Earlier lacustrine models for the ore depositional environment are not consistent with the biomarker evidence.

One of the remaining issues to be resolved is whether the ore sulfides formed within the sediment pile [9,15] or in the overlying water body [10]. Our results indicate similarities with the hydrothermal petroleums of the Guaymas Basin. There, hot waters permeated organic-rich sediments and generated oil with a distinctive chemistry. The very strong contrasts between absolute aromatic hydrocarbon abundances and distribution patterns between the north and south ends

of number 2 ore body (Fig. 3) are consistent with previous interpretations from base-metal ratios [13] that at 2 ore-body level the mineralizing fluid came from the north and cooled as it flowed south. It could perhaps be argued that lead and zinc sulfide formation occurred in a dense, bottom-hugging brine, and organic matter entrained in that brine and at the sediment–water interface was thermally altered in the water body. Among other things, this would require heat to be retained in the flowing brine along a distance of more than 1 km, beneath a cool, deep marine water body. It also predicts that the brine would have leached carbonate on the sea floor forming surfaces morphologically analogous to subaerial examples with micro-karst and scalloping [23]; no such surfaces are known.

In modern systems, such as the Guaymas Basin, the hydrothermally generated petroleum condenses in conduits and vugs as the temperature decreases. PAHs accumulate near the hotter vent chimneys, waxes at intermediate temperatures (20–80°C), with heavy oil in cool areas [24]. Plating of PAHs has also been noted in other mineral systems where hydrocarbons that precipitated from cooling solutions produced PAH minerals, such as curtisite, idrialite and pendletonite [25]. Although the PAHs at McArthur River appear to be distributed along a cooling trend, we do not observe other features associated with exhalation and rapid cooling, for example veins, tar mats and hydrocarbon-filled vugs. This suggests that precipitation of the hydrothermal PAHs occurred beneath the sediment–water interface, where cooling was slowed by the insulating properties of the sediments.

Distinctive heating regimes are associated with sub-basins containing Pb/Zn mineralization in the McArthur Basin. Late to overmature kerogen is found near major fault zones with maturity decreasing away from the faults [26]. The ore horizons within the McArthur River deposit itself have elevated T_{max} (>520°C) and values of 'random' Ro% up to 2.4% [1]. Sediments examined from above the ore zone exhibit maturities consistent with burial alone. Significantly, Ro analyses of unmineralized, texturally unmodified mudstone within ore also exhibit burial maturities expected for the sub-basin [9]. The existence of unmineralized zones within the ore horizons which do not exhibit elevated Ro% values, and which lie on the thermal burial trend, is considered to indicate that these zones were already impermeable to the ore-forming fluid at the time of mineralization [9]. This suggests that channeling of hot fluids along permeable horizons led to the interaction with organic matter within the silty turbidites. Acid-generating, ore-forming reactions would have generated additional porosity through carbonate dissolution [9]. Examination of ultrathin sections from siltstone units indicates loss of dolomite and the formation of micro-stylolites in the ore zones and re-deposition downstream of iron- and manganese-enriched carbonates (Fig. 4). As carbonates have retrograde solubilities, they are deposited either due to the loss of CO_2 or due to changes of pH. Because solubility products of Fe–Mn carbonates are lower than those of Ca–Mg-rich carbonates, the Fe–Mn carbonates precipitate earlier and closer to the site of dissolution.

An ore genesis model consistent with all available data is shown in Fig. 5 [1,8,9]. This is a refinement of the model of Williams [4,5]. The depth of ore formation is estimated to be $\sim$10–20 m below the sea floor, based on the preserved thickness of the uppermost unmodified outflow 'nodular carbonate' zone above the stratigraphically highest 8 ore body at McArthur River, which varies between 7 and 12 m in the region of intense drilling [9]. This is interpreted as preserving the original sedimentary relationships at the time of ore formation. Brine flow is envisaged to have been largely parallel to bedding, concentrated in the silty layers because of rapid loss of permeability in the muddy units during shallow burial. In zones of vertical leakage, the residual brine flowing out of the base-metal zone mixed with the overlying pore and interconnected basinal waters resulting in development of the second generation biogenic pyrite Py 2, plus secondary nodular carbonates, carbonate crusts and silica gels at the sediment–water interface. The turbidites within the ore sequence have not been reworked by wave action, indicating that deposition occurred below storm wave base. Our results do

not rule out the possibility that locally there could have been sufficient vertical leakage of the mineralizing fluids for some exhalative deposits to form. They do suggest, however, that this is not the predominant mechanism by which number 2 ore body formed. All eight ore bodies are very similar, and no spring-like mounds are known from the mine or in drill core (Damien Nihill, McArthur River Mines, personal communication).

5. Conclusion

The McArthur River deposit contains a suite of hydrocarbons significantly different from those in petroleum generated by burial maturation, but closely comparable to those of modern hydrothermal systems. The composition and pattern of distribution of the hydrocarbons strongly suggest a new model of ore formation with fluids much hotter (250–400°C) than previously predicted, at least where the PAHs were generated. At the suggested temperatures the fluids need not have been oxidized, the sulfide could have traveled with the metals, and relatively small volumes of fluid would have been required. The dissolution of carbonate to generate porosity and permeability would have been faster and more effective. Moreover, when the rising fluid encountered the carbonate-rich silts at shallow depths, rapid dissolution and the accompanying loss of pressure would cause inhalation and channeling of the fluids laterally along the silty beds. Such a model may be widely applicable to shale-hosted base-metal deposits.

Acknowledgements

We thank the McArthur River Mining Company for access to the mine and MIM Exploration for permission to sample core material, and in particular Steve Pevelly and Damien Nihill of MRM for help during fieldwork. Janet Hope and Ian Atkinson of Geoscience Australia are thanked for technical support. Bernd Simoneit and Subhash Jaireth made numerous helpful suggestions. Peter Southgate and Chris Boreham and journal reviewer Greg Webb are thanked for comments which improved the manuscript. We had helpful discussions with Neil Williams about the geology around McArthur River. M.R.W. thanks the Australian Research Council, NASA's exobiology program (through grants to A. H. Knoll and J. Farmer) and Macquarie University for financial support. J.C. and G.A.L. publish with the permission of the Chief Executive Officer of Geoscience Australia. *[BOYLE]*

References

[1] G.A. Logan, M.C. Hinman, M.R. Walter, R.E. Summons, Biogeochemistry of the 1640 Ma McArthur River (HYC) lead-zinc ore and host sediments, Northern Territory, Australia, Geochim. Cosmochim. Acta 65 (2001) 2317–2336.

[2] N.J.W. Croxford, S. Jephcott, The McArthur lead-zinc-silver deposit, N.T, Australas. Inst. Min. Metall. Proc. 243 (1972) 1–26.

[3] I.B. Lambert, K.M. Scott, Implications of geochmical investigations within and around the McArthur zinc-lead-silver deposit, North. Territ. J. Geochem. Explor. 2 (1973) 207–330.

[4] N. Williams, Studies of the base metal sulfide deposits at McArthur River, Northern Territory, Australia: I. The Cooley and Ridge deposits, Econ. Geol. 73 (1978) 1005–1035.

[5] N. Williams, Studies of the base metal sulfide deposits at McArthur River, Northern Territory, Australia: II. The sulfide and carbon relationships of the concordant deposit and their significance, Econ. Geol. 73 (1978) 1036–1056.

[6] D. Rye, N. Williams, Studies of the base metal sulfide deposits at McArthur River, Northern Territory, Australia: III. The stable isotope geochemistry of the H.Y.C., Ridge and Cooley deposits, Econ. Geol. 76 (1981) 826–842.

[7] I.H. Crick, Petrological and maturation characteristics of organic matter from the Middle Proterozoic McArthur Basin, Australia, Aust. J. Earth Sci. 39 (1992) 501–519.

[8] M.C. Hinman, Base metal mineralisation at McArthur River: Structure and kinematics of the HYC-Cooley zone at McArthur River, Northern Territory, Aust. Geol. Surv. Org. Record 1995/5, 1995.

[9] M.C. Hinman, Constraints, timing and processes of stratiform base metal mineralisation at the HYC Ag-Pb-Zn deposit, McArthur River. New developments in metallogenic research: The McArthur, Mount Isa, Cloncurry Minerals Province, James Cook University of North Queensland Economic Geology Research Unit, Extended Abstracts, Contrib. 56, 1996, pp. 56–59.

[10] R.R. Large, S.W. Bull, D.R. Cooke, P.J. McGoldrick, A

genetic model for the H.Y.C. deposit, Australia: Based on regional sedimentology, geochemistry, and sulfide-sediment relationships, Econ. Geol. 93 (1998) 1345–1368.
[11] J.H. Oehler, Microflora of the H.Y.C. Pyritic Shale Member of the Barney Creek Formation (McArthur Group), middle Proterozoic of northern Australia, Alcheringa 1 (1977) 314–349.
[12] J.H. Oehler, R.G. Logan, Microfossils, cherts, and associated mineralisation in the Proterozoic McArthur (H.Y.C.) lead-zinc-silver deposit, Econ. Geol. 72 (1977) 393–1409.
[13] R.G. Logan, The geology and mineralogical zoning of the H.Y.C. Ag-Pb-Zn deposit, McArthur River, Northern Territory, Australia, M.Sc. Thesis, Australian National University, Canberra, 1979.
[14] I.B. Lambert, The McArthur zinc-lead-silver deposit: features, metallogenesis and comparisons with other stratiform ore, in: K.H. Wolf (Ed.), Handbook of Stratiform and Stratabound Ore Deposits, Elsevier, Amsterdam, 1976, pp. 535–585.
[15] C.S. Eldridge, N. Williams, J.L. Walshe, Sulfur isotope variability in sediment-hosted massive sulfide deposits as determined using the ion microprobe SHRIMP: II. A study of the H.Y.C. deposit at McArthur River, Northern Territory Australia, Econ. Geol. 88 (1993) 1–26.
[16] O.E. Kawka, B.R.T. Simoniet, Polycylic aromatic hydrocarbons in hydrothermal petroleums from the Guaymas Basin spreading centre, Appl. Geochem. 5 (1990) 17–27.
[17] B.R.T. Simoneit, Lipid/bitumen maturation by hydrothermal activity in sediments of Middle Valley, Leg 139, in: M.J. Mottl, E.E. Davis, A.T. Fisher, J.F. Slack (Eds.), Proc. ODP Sci. Results 139 (1994) 447–465.
[18] M.C. Warner, Geochemical characterization of sedimentary organic matter and hydrothermal petroleum in the black shale-hosted Zn-Pb deposit at Red Dog Mine, Western Brooks Range, Alaska, Ph.D. Thesis, Indiana University, 1998.
[19] W. Puttman, H.W. Hagemann, C. Merz, S. Speczik, Influence of organic material on mineralization processes in the Permian Kupferschiefer Formation, Poland, Org. Geochem. 13 (1988) 357–363.
[20] W. Puttman, H. Heppenheimer, R. Diedel, Accumulation of copper in the Permian Kupferschiefer: A result of post-depositional redox reactions, Org. Geochem. 16 (1990) 1145–1156.
[21] R.E. Summons, T.G. Powell, C.J. Boreham, Petroleum geology and geochemistry of the Middle Proterozoic McArthur Basin, Northern Australia: III. Composition of extractable hydrocarbons, Geochim. Cosmochim. Acta 52 (1988) 1747–1763.
[22] S.W. Bull, Sedimentology of the Palaeoproterozoic Barney Creek Formation in DDH Bureau of Mineral Resources (BMR) McArthur 2, Southern McArthur Basin, Northern Territory, Australia, Aust. J. Earth Sci. 45 (1998) 21–31.
[23] J.F. Read, G.A. Grover, Scalloped planar erosion surfaces, Middle Cambrian limestones, Virginia: analogues of tidal rock platforms, J. Sediment. Petrol. 47 (1977) 956–972.
[24] B.R.T. Simoneit, Petroleum generation, an easy and widespread process in hydrothermal systems: an overview, Appl. Geochem. 5 (1990) 3–15.
[25] M. Blumer, Curtisite, idrialite and pendletonite, polycyclic aromatic hydrocarbon minerals: their composition and origin, Chem. Geol. 16 (1975) 245–256.
[26] I.H. Crick, C.J. Boreham, A.C. Cook, T.G. Powell, Petroleum geology and geochemistry of Middle Proterozoic McArthur Basin, northern Australia II: assessment of source rock potential, Am. Assoc. Pet. Geol. 72 (1988) 1495–1514.